

EAGAN: Efficient Two-stage Evolutionary Architecture Search for GANs

Guohao Ying,^{1*} Xin He,^{2*} Bin Gao,³ Bo Han,² Xiaowen Chu^{2†}

¹ University of Southern California

² Hong Kong Baptist University

³ National University of Singapore

gying@usc.edu, {csxinhe,bhanml,chuxw}@comp.hkbu.edu.hk, bingao@comp.nus.edu.sg

Abstract

Generative Adversarial Networks (GANs) have been proven hugely successful in image generation tasks, but GAN training has the problem of instability. Many works have improved the stability of GAN training by manually modifying the GAN architecture, which requires human expertise and extensive trial-and-error. Thus, neural architecture search (NAS), which aims to automate the model design, has been applied to search GANs on the task of unconditional image generation. The early NAS-GAN works only search generators for reducing difficulty. Some recent works have attempted to search both generator (G) and discriminator (D) to improve GAN performance, but they still suffer from the instability of GAN training during the search. To alleviate the instability issue, we propose an efficient two-stage evolutionary algorithm (EA) based NAS framework to discover GANs, dubbed **EAGAN**. Specifically, we decouple the search of G and D into two stages and propose the weight-resetting strategy to improve the stability of GAN training. Besides, we perform evolution operations to produce the Pareto-front architectures based on multiple objectives, resulting in a superior combination of G and D. By leveraging the weight-sharing strategy and low-fidelity evaluation, EAGAN can significantly shorten the search time. EAGAN achieves highly competitive results on the CIFAR-10 (IS=8.81±0.10, FID=9.91) and surpasses previous NAS-searched GANs on the STL-10 dataset (IS=10.44±0.087, FID=22.18).

1 Introduction

Generative adversarial networks (GANs) (Goodfellow et al. 2014) have obtained remarkable achievements in image generation. Researchers have made great efforts to design various architectures of GANs (Radford, Metz, and Chintala 2016; Brock, Donahue, and Simonyan 2019; Zhang et al. 2019). However, due to the instability of the GAN training, designing GANs by humans usually requires much expertise and laborious trial-and-error.

Recently, neural architecture search (NAS) has successfully discovered superior models that outperform human-designed models in various tasks (Elsken, Metzen, and Hutter 2018; He, Zhao, and Chu 2021). Many studies have used

*equal contribution

†Corresponding author

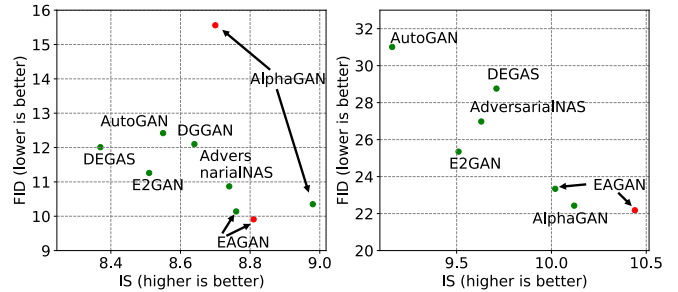


Figure 1: IS versus FID on the CIFAR-10 (left) and STL-10 (right) datasets. The closer to the bottom right corner, the better the model performance. The green and red points indicate the results of only searching generators and searching both generators and discriminators, respectively. (Best viewed in color)

NAS to discover superior GANs that surpass hand-crafted ones, but there are still some under-explored problems. Early NAS-GAN works only search generator (G) with a fixed architecture of discriminator (D) to reduce search difficulty, but this limits the generator performance since GANs highly depend on the constant competition between G and D. Some recent works have explored to search both G and D to improve GAN performance, while they suffer from the instability of GAN training. AdversarialNAS (Gao et al. 2020) is the first gradient descent (GD)-based NAS-GAN work that proposes an adversarial loss function to search G and D simultaneously in a differentiable manner, but the architectures of G and D are deeply coupled, which increases combinatorial complexity and the instability of GAN training. The ablation experiment of a subsequent GD-based NAS-GAN work (Tian et al. 2020a) shows that simultaneously searching both G and D hampers the search of optimal GANs. DGGAN alleviates instability by progressively growing G and D in an alternating way but takes 580 GPU days to search on the CIFAR-10 dataset (Krizhevsky, Hinton et al. 2009).

In this paper, we propose an efficient two-stage Evolutionary Architecture search framework for Generative Adversarial Networks (**EAGAN**) on the unconditional image generation tasks. First, to alleviate the instability of GAN training during search, we decouple the search of G and D into two stages. In stage-1, we fix the architecture

Method	Type	Discriminator?	Multi-objective?	Evaluation
AGAN (Wang and Huan 2019)	RL	×	×	IS
AutoGAN (Gong et al. 2019)		×	×	IS
E2GAN (Tian et al. 2020b)		×	✓	Linear(IS,FID)†
DEGAS (Doveh and Giryas 2019)	GD	×	×	Adversarial loss
AdversarialNAS (Gao et al. 2020)		✓	×	Adversarial loss
AlphaGAN (Tian et al. 2020a)		✓	×	Adversarial loss
COEGAN (Costa, Lourenço, and Machado 2019)	EA	✓	×	FID
EGAN (Wang et al. 2019)		×	✓	Linear(quality,diversity)†
EAGAN		✓	✓	Pareto-front(IS,FID,#size)‡

Table 1: Comparison of our EAGAN and the existing NAS-GAN methods. The third column indicates whether the method supports searching discriminators. † indicates a linear combination of metrics. ‡ indicates the Pareto-front of multiple metrics.

of discriminator and only search generators. Each generator is paired with the same discriminator, that is, the candidate generators and the fixed discriminator are in a *many-to-one* relationship. In stage-2, the best generator of stage-1 is used to provide supervision signals for searching discriminators. Specifically, we create multiple copies of the best generator architecture of stage-1 in stage-2, and each generator copy is paired with a different discriminator and trained independently. Thus, the generators and candidate discriminators of stage-2 are in a *many-to-many* relationship. A potential problem in stage-2 is that if some generators have mode collapse, the corresponding discriminators cannot be evaluated correctly because they are indirectly assessed via generators. To solve this problem, we propose a *weight-resetting* strategy, where all generators inherit the weights of the best generator of the previous search round before a new search round starts. The results show that our weight-resetting strategy can effectively stabilize GAN searching.

Second, to efficiently find the superior combination of G and D, we choose the evolutionary algorithm (EA) based NAS method based on the following considerations. 1) *EA is a global optimization method and robust to initial states* (Heitzinger 2002). According to (Real et al. 2019; He, Zhao, and Chu 2021), EA-based NAS usually achieves better results than other types of NAS methods on the image classification tasks. However, the search cost of EA-based methods is much expensive, e.g., (Real et al. 2019) takes 3,150 GPU days to search on the CIFAR-10 dataset. To alleviate resource consumption, we adopt the *weight-sharing* strategy (Pham et al. 2018) and the *low-fidelity* method (Chrabaszcz, Loshchilov, and Hutter 2017) to reduce the search time on the CIFAR-10 dataset to 1.2 GPU days. 2) *EA is good at solving multi-objective optimization problems*. Since there is currently no consensus as to which metric best reflects the performance of GANs (Borji 2019), it is necessary to consider multiple conflicting metrics, such as Inception Score (IS) (Salimans et al. 2016) that measures the quality and diversity of the generated images, and Fréchet Inception Distance (FID) (Heusel et al. 2017) that captures the similarity between the generated images and real images. As summarized in Tab. 1, GD-based NAS-GAN optimize architectures via loss value, which cannot reflect the status of GANs (Brock, Donahue, and Simonyan 2019; Grnarova et al. 2019). COEGAN (Costa, Lourenço, and Machado 2019) is also an EA-based NAS-GAN method.

It uses adversarial loss value to monitor discriminator performance, but the results evidence that loss value cannot ensure a proper evolution of the architectures. Although E2GAN (Tian et al. 2020b) and EGAN (Wang et al. 2019) use a linear combination of metrics for evaluation, they introduce an additional ratio coefficient, the optimal value of which is hard to find, thus increasing searching difficulty. To this end, we adopt a widely used selection method, *non-dominated sorting* strategy (Deb et al. 2000), to produce the Pareto-front architectures under three different objectives: IS, FID, and model size.

To sum up, our main contributions are three-fold.

1. We greatly reduce the instability of GAN training by decoupling the search of generator and discriminator into two stages. To avoid mode collapse, we propose a general weight-resetting strategy in stage-2 to obtain fair and unbiased evaluation of different discriminators.
2. With the weight-sharing and low-fidelity strategies, EAGAN can efficiently search GANs within 1.2 GPU days on the CIFAR-10 dataset.
3. EAGAN can discover superior GAN architectures on the CIFAR-10 dataset. The searched GAN has advanced transferability and surpasses all previous NAS-searched GANs on the STL-10 dataset (Coates, Ng, and Lee 2011).

2 Related Work

2.1 Generative Adversarial Networks

Generative Adversarial Networks (GANs) are first proposed in (Goodfellow et al. 2014) and have been widely used in various generation and synthesis tasks. A GAN comprises a generator (G) that generates plausible new data and a discriminator (D) that aims to distinguish the generator’s fake data from real data. Thus, G and D play a min-max game with each other, leading to the instability of GAN training, such as mode collapse and gradient vanishing. Many efforts have been made on multiple fronts to alleviate these problems (Bissoto, Valle, and Avila 2019), such as loss functions (Arjovsky, Chintala, and Bottou 2017; Wang, Sun, and Halgamuge 2019; Hjelm et al. 2017; Mao et al. 2017), normalization and constraint (Gulrajani et al. 2017; Miyato et al. 2018a), conditional techniques (Odena, Olah, and Shlens 2017; Karras, Laine, and Aila 2019), and validation

methods (Salimans et al. 2016; Heusel et al. 2017). Besides, architecture enhancements have been proven effective to improve GANs performance in many works (Radford, Metz, and Chintala 2016; Brock, Donahue, and Simonyan 2019; Zhang et al. 2019; Karras et al. 2018), but they all require much expertise and trial-and-error.

2.2 Neural Architecture Search for GANs

Neural architecture search (NAS) that aims at automatic architecture design has achieved remarkable results in various fields (Elsken, Metzen, and Hutter 2018). There are mainly four approaches in NAS: reinforcement learning (RL) (Zoph and Le 2016; Zoph et al. 2018; Pham et al. 2018), gradient descent (GD) (Liu, Simonyan, and Yang 2019; Wu et al. 2019; Xu et al. 2020), surrogate model-based optimization (SMBO) (Liu et al. 2018), and evolutionary algorithm (EA) based methods (Real et al. 2019; Yang et al. 2020; Real et al. 2017; Liu et al. 2017). Many works have applied NAS to search GANs, as summarized in Tab. 1. AGAN (Wang and Huan 2019) and AutoGAN (Gong et al. 2019) are among the first RL-based NAS methods to search GANs, but they only use IS as the reward to guide the search. E2GAN (Tian et al. 2020b) is rewarded by a linear combination of IS and FID. However, these RL-based NAS-GAN studies only search generators. The second group is gradient descent (GD) based methods that apply softmax function to relax the discrete search space to allow differential optimization of architectures. E.g., DEGAS (Doveh and Giryes 2019) uses the generative latent optimization (GLO) (Bojanowski et al. 2018) framework to search generators. Although AdversarialNAS (Gao et al. 2020) proposes a reconstruction adversarial loss function to search the architectures of generator and discriminator simultaneously, the architectures of the generators and discriminators are deeply coupled, which further aggravates the instability of GAN training. AlphaGAN (Tian et al. 2020a) targets at finding pure Nash equilibrium of generator and discriminator and exploits a fully differentiable search framework by formalizing a bi-level min-max optimization problem. The third category is the evolutionary algorithm (EA) based methods, which are the most relevant to our proposed method. EGAN (Wang et al. 2019) only searches generator and doesn't perform well on the CIFAR-10 dataset. COEGAN (Costa, Lourenço, and Machado 2019) searches both G and D, but its experiment lacks generality as it only searches on a very small search space (up to 4 layers of convolution or linear layers) using the MNIST dataset (LeCun et al. 1998).

3 Methods

3.1 Two-stage Searching GANs

Motivation GAN training is notoriously unstable and prone to collapse; thus, the early NAS-GAN methods only search generator (G) with a fixed architecture of discriminator (D). Although there have been some studies on searching both G and D, there are still some unresolved problems. For example, AdversarialNAS (Gao et al. 2020) searches G and D simultaneously in a differentiable way, but this mechanism results in highly coupled architectures of G and D and

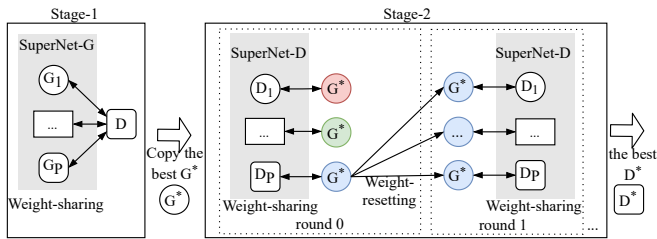


Figure 2: The pipeline of EAGAN. Different shapes and colors indicate different architectures and weights, respectively. In stage-1, a fixed discriminator guides the search of the best generator G^* . In stage-2, each discriminator is paired with an independent generator having the same architecture as G^* . Before each round of stage-2, we weight-reset all generators with the weights of the best generator of the previous round. (Best viewed in color)

hence amplifies the instability of GAN training. The ablation study in (Tian et al. 2020a) has also demonstrated that simultaneously searching G and D would potentially increase the negative effect of inferior discriminators and hinder finding the optimal GANs. Liu et al. (Liu et al. 2021) propose to progressively grow the architectures of G and D in an alternating fashion. However, their method suffers from huge computational costs (580 GPU days on the CIFAR-10 dataset). COEGAN (Costa, Lourenço, and Machado 2019) is very relevant to our work, which also uses an evolutionary algorithm to search G and D in two separate groups of architectures (called populations). Since their two populations' architectures are coupled during search, to reduce the difficulty of searching, COEGAN only explores a very simple search space and experiments on a small dataset (MNIST). The final results show that COEGAN fails to outperform the previous human-designed GANs. Based on the above reviews, we believe that coupling G and D is not conducive to searching for the optimal GAN. Therefore, we propose a two-stage scheme to decouple the search of G and D. Fig. 2 presents the pipeline of our two-stage EAGAN, and Alg. 1 summarizes the detailed process.

Stage-1: Generator Searching The search stage involves R rounds, and each round comprises E epochs of weights training and one architecture evolution. During each round of stage-1, a group of P generators (called *population-G* \mathcal{A}_G) is trained and updated. Specifically, these P generators are paired with the same discriminator having a fixed architecture. This mechanism can bring two benefits. First, it can avoid the situation that the discriminator becomes much stronger than the generator because the discriminator is trained with various generators, which can be viewed as an ensemble method to some extent. Second, since different generators are trained with the same discriminator, they can be evaluated fairly, and hence we can find the Pareto-front generators from the population without bias. To make sure each generator is trained equally, for each training batch, we uniformly draw a generator from the population and train it with the fixed discriminator (Alg. 1 lines 4 to 10).

Stage-2: Discriminator Searching with Weight-resetting After stage-1, we can obtain the best generator G^* and use it

to provide supervision signals to help search the corresponding best discriminator in stage-2. In stage-1, all candidate generators are paired with the same discriminator. However, we cannot simply apply the same strategy in stage-2 because we use IS and FID to indirectly assess the discriminator performance, and these two metrics are calculated based on the generator. In other words, if all discriminators are paired with the same generator, we cannot compare these discriminators. A possible solution is to pair each discriminator with an independent generator, which has the same architecture as G^* . However, a potential problem with this solution is that, with constant training and searching, the weights of each generator may be optimized in different directions, and some of them may have mode collapse. This will result in an unfair and biased evaluation for the discriminators paired with those collapsed generators.

To alleviate the above problem, we propose the weight-resetting strategy. Concretely, in stage-2, we create P copies of the best generator architecture (G^*) of stage-1 and pair them with P different discriminators (called *population-D* \mathcal{A}_D) in each search round. For the first round, all generators are initialized with the weights of G^* . We uniformly train a pair of generator and discriminator in each training batch, ensuring each GAN equally trained (Alg. 1 lines 21 to 27). After training, the generators that are initialized with the same weight will have different performance and weights (indicated by different colors in Fig. 2). We select the best generator among P generator copies via a selection algorithm described in Section 3.3, and set its weights to the initial weights of all generators in the next round. In summary, the *weight-resetting* strategy brings two benefits. First, it can eliminate the negative impact of those generators with mode collapse in stage-2. Second, in each round, different discriminators can be fairly evaluated without bias.

3.2 Search Space and Weight-sharing

To enable a fair comparison, we use the same search space as (Gao et al. 2020) since it also searches both generators and discriminators. The search space comprises two super networks (see Fig. 3): SuperNet-G and SuperNet-D. In stage-1, all generators are searched from SuperNet-G. In stage-2, all discriminators are searched from SuperNet-D.

SuperNet-G \mathcal{N}_G comprises a fully-connected (FC) layer and three Up-Cells. Each cell contains five ordered nodes (0-4), where Node 0 is the output of the previous cell or the input data. The edges between nodes represent different predefined operations. Specifically, the edges U_0 and U_1 indicate up-sampling operations selected from {Nearest Neighbor Interpolation, Bilinear Interpolation, Transposed Conv 3×3 }. The rest edges (U_2 to U_6) indicate normal operations selected from 7 candidates keeping feature size (stride=1): None (no connection between two nodes), Skip-connection, Conv $\{1 \times 1, 3 \times 3, 5 \times 5\}$ with dilation of 1, and Conv $\{3 \times 3, 5 \times 5\}$ with dilation of 2.

SuperNet-D \mathcal{N}_D comprises three Down-Cells and an FC layer. The Down-Cell is the inverted structure of the Up-Cell. The only difference is that the edges D_5 and D_6 are down-sampling operations (stride=2) among 6 candidates: Average Pooling, Max Pooling, Conv $\{3 \times 3, 5 \times 5\}$ with

Algorithm 1: EAGAN.

Input: SuperNet-G \mathcal{N}_G , SuperNet-D \mathcal{N}_D , population-G \mathcal{A}_G , population-D \mathcal{A}_D , population size P , criterion \mathcal{H}_G and \mathcal{H}_D , multi-objective set \mathcal{F} , total search rounds R , each round contains E epochs of training.

Output: G^* and D^*

```

1  $D \leftarrow$  Initialize a discriminator
2  $\mathcal{A}_G^{(0)} = \{\mathcal{N}_{G_1}^{(0)}, \dots, \mathcal{N}_{G_P}^{(0)}\} \leftarrow$  Warm-up( $\mathcal{N}_G, D$ )
   for  $r=0:R-1$  do
3     for  $e=0:E-1$  do
4         for batch  $x = \{x_1, \dots, x_m\}$  in training set do
5             Sample noise data  $z = \{z_1, \dots, z_m\}$ 
6             Uniformly sample  $\mathcal{N}_{G_i}^{(r)}$  from  $\mathcal{A}_G^{(r)}, i \in [1, P]$ 
7             Update weights of  $D$  by gradient
                $\frac{1}{m} \nabla \sum_{j=1}^m \mathcal{H}_D(x_j, z_j | \mathcal{N}_{G_i}^{(r)}, D)$ 
8             Sample noise data  $z = \{z_1, \dots, z_m\}$ 
9             Update weights of  $\mathcal{N}_{G_i}^{(r)}$  by gradient
                $\frac{1}{m} \nabla \sum_{j=1}^m \mathcal{H}_G(z_j | \mathcal{N}_{G_i}^{(r)}, D)$ 
10        end
11    end
12     $\mathcal{A}_G^{(r)} \leftarrow$  Select Pareto-front based on  $\mathcal{F}$ 
13     $\mathcal{A}_G^{(r)} \leftarrow$  Crossover&Mutation( $\mathcal{A}_G^{(r)}$ )
14  end
15   $G^* \leftarrow$  the best generator
16   $\mathcal{A}_D^{(0)} = \{\mathcal{N}_{D_1}^{(0)}, \dots, \mathcal{N}_{D_P}^{(0)}\} \leftarrow$  Warm-up( $G^*, \mathcal{N}_D$ )
17  Initialize  $P$  GANs  $\{(G_i, \mathcal{N}_{D_i}^{(0)}), i \in [1, P]\}$ , where  $G_i$  has
   the same architecture as  $G^*$ 
18  for  $r=0:R-1$  do
19      Weight-resetting  $W_{G_1} = \dots = W_{G_P} = W_{G^*}$ 
20      for  $e=0:E-1$  do
21          for batch  $x = \{x_1, \dots, x_m\}$  in training set do
22              Sample noise data  $z = \{z_1, \dots, z_m\}$ 
23              Uniformly sample  $\mathcal{N}_{D_i}^{(r)}$  from  $\mathcal{A}_D^{(r)}, i \in [1, P]$ 
24              Update weights of  $\mathcal{N}_{D_i}^{(r)}$  by gradient
                  $\nabla \sum_{j=1}^m \mathcal{H}_D(x_j, z_j | G_i, \mathcal{N}_{D_i}^{(r)})$ 
25              Sample noise data  $z = \{z_1, \dots, z_m\}$ 
26              Update weights of  $G_i$  by gradient
                  $\nabla \sum_{j=1}^m \mathcal{H}_G(z_j | G_i, \mathcal{N}_{D_i}^{(r)})$ 
27          end
28      end
29       $\mathcal{A}_D^{(r)} \leftarrow$  Select Pareto-front based on  $\mathcal{F}$ 
30       $W_{G^*} \leftarrow$  the generator weights of the best GAN
31       $\mathcal{A}_D^{(r)} \leftarrow$  Crossover&Mutation( $\mathcal{A}_D^{(r)}$ )
32  end
33   $D^* \leftarrow$  the best discriminator

```

dilation of 1, and Conv $\{3 \times 3, 5 \times 5\}$ with dilation of 2.

Weight-sharing The early NAS methods (Real et al. 2019; Zoph and Le 2016) train all sub-networks from scratch to find the best one, but they required a lot of resources. To

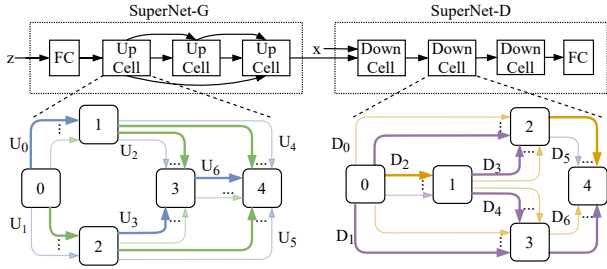


Figure 3: The search space of EAGAN. U_0 and U_1 are up-sampling operations, D_5 and D_6 are down-sampling operations, and the other edges are normal operations.

address this problem, many subsequent NAS methods (Liu, Simonyan, and Yang 2019; Pham et al. 2018; Yang et al. 2020) use the weight-sharing strategy to allow all sub-networks to inherit each other’s weights without needing to be trained from scratch, which greatly improves search efficiency. Therefore, we also adopt this method in our work.

To avoid abuse of notations, we use \mathcal{N} to refer to both SuperNet-G \mathcal{N}_G and SuperNet-D \mathcal{N}_D . The SuperNet \mathcal{N} contains all child networks \mathcal{N}_i (individuals) that share weights among each other. Denote the loss of individual \mathcal{N}_i as L_i , and the weights of the SuperNet as W . The gradient of SuperNet loss L with respect to W is $\nabla_W L = \frac{1}{N} \sum_{i=1}^N \nabla_{W_i} L_i = \frac{1}{N} \sum_{i=1}^N \frac{\partial L_i}{\partial W_i}$, where W_i is the weights of individual \mathcal{N}_i , and N is the total number of individuals. However, it is not practical to accumulate all individuals’ gradients for each batch. Therefore, we borrow the idea of stochastic gradient descent and use a mini-batch of individuals (i.e., the population size P) to update shared weights. Besides, in our experiments, we find that randomly sampling one sub-network and updating its weights per batch can also effectively update SuperNet weights, instead of sampling P sub-networks, which further improves the search efficiency.

3.3 Evolution

Encoding The architectures of SuperNet-G and SuperNet-D are built by stacking multiple Up-Cells or Down-Cells. The operations on the edges determine each cell. We encode each operation by a one-hot sequence, e.g., the bilinear interpolation is encoded as $[0,1,0]$ in three upsampling operations. Accordingly, each architecture can be encoded as a set of one-hot sequences. In other words, searching the architecture is transformed to searching a set of one-hot encoding sequences for different cells.

Selection We adopt non-dominated sorting strategy (Deb et al. 2000) to obtain the Pareto-front architectures from the population (\mathcal{A}_G or \mathcal{A}_D). The selected architectures are used to generate offspring by crossover and mutation. \mathcal{N}_i is dominated by \mathcal{N}_j when Eq. 1 satisfies.

$$\begin{aligned} \mathcal{F}_k(\mathcal{N}_i) &\geq \mathcal{F}_k(\mathcal{N}_j) \quad \forall k \in \{1, \dots, K\} \\ \mathcal{F}_k(\mathcal{N}_i) &> \mathcal{F}_k(\mathcal{N}_j) \quad \exists k \in \{1, \dots, K\} \end{aligned} \quad (1)$$

where \mathcal{F}_k indicates the objective. Here, we use three ($K =$

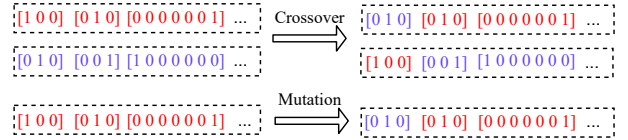


Figure 4: Examples of crossover and mutation. For simplicity, we only show the one-hot encoding sequences of U_0 to U_2 in Fig. 3.

3) objectives: model size, FID, and $\frac{1}{IS}^1$. According to the number of times each individual is dominated by other individuals, we can split P individuals into l different non-dominated sorting lists $\Omega = \{\Omega_0, \Omega_1, \dots, \Omega_{l-1}\}$, where $l-1$ is the maximum dominated number. For instance, the individuals in the Ω_0 list are not dominated by any other individuals, i.e., they perform best on all objectives.

Crossover Since each architecture is encoded by a set of one-hot sequences and all child architectures share weights among each other, the basic units of both crossover and mutation are one-hot sequences. Given the non-dominated sorting lists Ω , we select the top half ($\frac{P}{2}$) of architectures as parents. We randomly select two parents and perform crossover until we generate $\frac{P}{2}$ new architectures. The selected two parent individuals randomly exchange only one operation. Fig. 4 gives an example of crossover, where two parents exchange only the operation on edge U_0 in Fig. 3.

Mutation To enhance the diversity of the population, we perform mutation on child individuals with a probability of 0.5. Specifically, we randomly sample only one edge and change the position of 1 in its one-hot sequence. Fig. 4 shows an example of mutation, where the operation on the edge U_0 in Fig. 3 is mutated from the nearest neighbor interpolation ($[1,0,0]$) to bilinear interpolation ($[0,1,0]$).

4 Experiments

4.1 Datasets

Following the previous NAS-GAN works (Gong et al. 2019; Gao et al. 2020), we run experiments on the CIFAR-10 (Krizhevsky, Hinton et al. 2009) and STL-10 (Coates, Ng, and Lee 2011) datasets. CIFAR-10 consists of 50,000 training images and 10,000 test images with 32×32 resolutions. STL-10 contains 100,500 images with 96×96 resolutions, but we resize them to 48×48 as previous NAS-GAN setting.

4.2 Implementation Settings

Our code is based on PyTorch (Paszke et al. 2019) and will be open-sourced. We use one NVIDIA Tesla V100 GPU and take only 1.2 GPU days to finish the search.

Warm-up Stage Since all candidate operations share weights among each other, if we directly initialize a population, the most frequently used operations are trained more often and tend to be selected with a higher probability in the later search process. To alleviate this problem, we set up a warm-up stage for two search stages. Specifically, in

¹The higher the IS value, the better the model performance

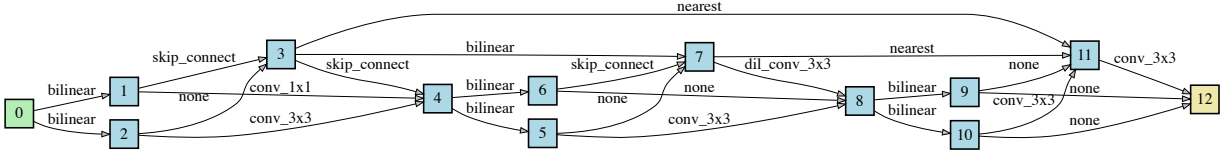


Figure 5: The architecture of the searched generator.

the warm-up stage, each candidate operation is selected uniformly and hence trained equally. The warm-up stage has 50 epochs. After that, we randomly sample P individuals to form the first population.

Two-stage Search For two search stages, we use hinge loss (Miyato et al. 2018b) and Adam optimizer (Kingma and Ba 2014) with an initial learning rate of 0.0002. The number of searching rounds is 15, each containing 10 epochs. The noise data is sampled from the Gaussian distribution. During each round, a population of 32 individuals is trained and evolved. The batch sizes for generator and discriminator are 40 and 80, respectively. Besides, we adopt a low-fidelity evaluation strategy to improve search efficiency. Specifically, the number of images used to calculate FID and IS is reduced to 5,000, which greatly reduce the evaluation time and keep the performance of the searched architectures. Stage-1 and stage-2 take 0.8 and 0.4 GPU days, respectively.

Fully-train Stage After the search, we fully train the best-performing GAN (G^* , D^*) from scratch. For the CIFAR-10 dataset, the batch size and learning rate are the same as the search stage, but the total number of training epochs is 600. For the STL-10 dataset, the batch size and the learning rate are 128 and 0.0003 for the generator, and 64 and 0.0002 for the discriminator, respectively. Following the previous NAS-GAN works (Gao et al. 2020; Gong et al. 2019), we generate 50,000 images to calculate IS and FID metrics.

4.3 Results and Analysis

Search only Generator Our searched generator is shown in Fig. 5, from which we can summarize:

1. Bi-linear operation is preferred for up-sampling. The same observation has also been presented in previous NAS-GAN works (Tian et al. 2020b; Gao et al. 2020).
2. Convolution operations with kernel size larger than three are not chosen in our searched generator. This result is consistent with the common model design paradigm.
3. The whole search stage is optimized under multiple objectives (IS, FID, and model size). Fig. 5 shows that there are 6 “None” operations and 3 “skip-connect” operations among 15 total normal operations. These operations greatly reduce the model size. Besides, the results in Tab. 2 show that EAGAN achieves good performance on both CIFAR-10 and STL-10 datasets, which demonstrates the effectiveness of EAGAN’s multi-objective optimization.

Tab. 2 gives the comparisons with previous state-of-the-art (SOTA) methods. From the table, we can see that when

searching only generators, our EAGAN can find a much better generator than AdversarialNAS (Gao et al. 2020) in the same search space, which implies that the evolutionary algorithm can effectively find excellent generators under multiple objectives (IS, FID, and model size). Compared with the existing NAS-GAN works, our discovered generator achieves a highly competitive FID score (10.14) and IS result (8.76 ± 0.09) on the CIFAR-10 dataset. In terms of IS, there is a certain gap between our method and BigGAN (Brock, Donahue, and Simonyan 2019). The possible reason is that BigGAN introduces category information as input into the generator’s architecture, while our generator only receives noise data. As a future work, we can try to improve the GAN performance by incorporating category information into the search space. We also evaluate the transferability of the searched generator on the STL-10 dataset. The results in Tab. 2 show that our searched generator has strong generalization ability as it achieves remarkable results of IS (10.02 ± 0.11) and FID (23.34).

Search both Generator and Discriminator In stage-2, we use the best generator of stage-1 to provide supervision signals for searching the Pareto-front of discriminators, from which we further select the most proper discriminators for the CIFAR-10 and STL-10 datasets, respectively. Similar to the searched generator, the searched architectures of discriminators (see Appendix) also have many “None” and “Skip-connect” operations due to the objective of model size. From Tab. 2, we can see that the existing NAS-GAN methods cannot guarantee to find excellent GANs under both two search scenarios: (a) searching only generators and (b) searching both generators and discriminators. For example, AdversarialNAS (Gao et al. 2020) does not perform well in scenario (a), and AlphaGAN (Tian et al. 2020a) suffers from instability in scenario (b) as its performance drops significantly from (IS= 8.89 ± 0.09 , FID= 10.35) to (IS= 8.70 ± 0.11 , FID= 15.56) when searching generators and discriminators. Our EAGAN can well balance these two search settings. The results show that the searched discriminator can further facilitate the performance of the generator discovered in stage-1. Specifically, we achieve a higher IS value (8.81 ± 0.10) and the best FID (9.91) on the CIFAR-10 dataset. Besides, our EAGAN achieves remarkable results (IS= 10.44 ± 0.08 , FID= 22.18) on the STL-10 dataset, which outperforms all other NAS-searched GANs. In Appendix Fig. 1, we randomly present 50 images generated by generators trained on the CIFAR-10 and the STL-10 dataset without cherry-picking, respectively. The generated images

Method	Search Method	GPU Days	CIFAR-10		STL-10	
			IS \uparrow	FID \downarrow	IS \uparrow	FID \downarrow
DCGANs (Radford, Metz, and Chintala 2016)	Manual	-	6.64 \pm 0.14	37.7	-	-
WGAN-GP (Gulrajani et al. 2017)			7.86 \pm 0.07	29.3	-	-
Progressive GAN (Karras et al. 2018)			8.80 \pm 0.05	18.33	-	-
SN-GAN (Miyato et al. 2018a)			8.22 \pm 0.05	21.7	9.16 \pm 0.12	40.1
ProGAN (He et al. 2018)			7.75	24.60	8.87 \pm 0.09	46.74
Improv MMD GAN(Wang, Sun, and Halgamuge 2019)			8.29	16.21	9.34	37.63
BigGAN (Brock, Donahue, and Simonyan 2019)			9.22	14.73	-	-
AGAN (Wang and Huan 2019)	RL	1200	8.29 \pm 0.09	30.5	9.23 \pm 0.08	52.7
AutoGAN (Gong et al. 2019)		2	8.55 \pm 0.10	12.42	9.16 \pm 0.12	31.01
E2GAN (Tian et al. 2020b)		0.3	8.51 \pm 0.13	11.26	9.51 \pm 0.09	25.35
DEGAS (Doveh and Giryes 2019)	GD	1.167	8.37 \pm 0.08	12.01	9.71 \pm 0.11	28.76
AlphaGAN (Tian et al. 2020a)		0.13	8.98 \pm 0.09	10.35	10.12 \pm 0.13	22.43
AlphaGAN (Tian et al. 2020a) (G+D)		-	8.70 \pm 0.11	15.56	-	-
AdversarialNAS (Gao et al. 2020)		1	7.86 \pm 0.08	24.04	8.52 \pm 0.05	38.85
AdversarialNAS (Gao et al. 2020) (G + D)		1	8.74 \pm 0.07	10.87	9.63 \pm 0.19	26.98
DGGAN (Liu et al. 2021)	Heuristic	580	8.64 \pm 0.06	12.10	-	-
EGAN (Wang et al. 2019)	EA	1.25	6.9 \pm 0.09	-	-	-
Our EAGAN		0.8	8.76 \pm 0.09	10.14	10.02 \pm 0.11	23.34
Our EAGAN (G+D)		1.2	8.81 \pm 0.10	9.91	10.44\pm0.08	22.18

Table 2: Performance comparison with hand-crafted and NAS-designed GANs on the CIFAR-10 and STL-10 datasets. “(G+D)” indicates the results when searching both generators and discriminators. The other NAS-GAN results are obtained when searching only generators.

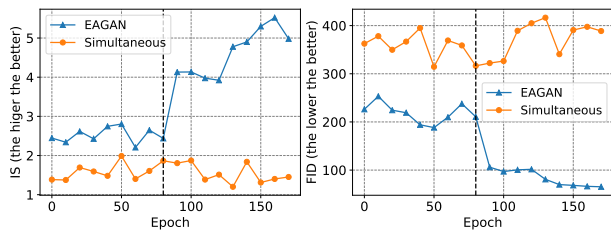


Figure 6: The curves of IS and FID during search. “Simultaneous” indicates searching generators and discriminators simultaneously. The blue curves on the left and right sides of the dashed line represent the results of stage-1 and stage-2 of EAGAN, respectively. (Best viewed in color)

are of rich diversity and high quality.

4.4 Ablation Study

Two-stage Searching We explore the effectiveness of two-stage searching scheme. We implement the simultaneous search strategy as the baseline, i.e., G and D evolve simultaneously to generate new offspring for each search round. For a fair comparison, the baseline uses the same evolution operations and search space as EAGAN. The IS and FID during search are presented in Fig. 6. We can see that the IS and FID of EAGAN fluctuate in stage-1, but its overall performance is obviously better than the baseline. In stage-2 of searching discriminators, the performance of EAGAN is significantly improved, while the baseline still fails to converge.

Weight-resetting Strategy Second, we study the influence of weight-resetting strategy on the CIFAR-10 dataset. Fig. 7 presents curves of IS and FID during search with and without the weight-resetting (WR) strategy. From the fig-

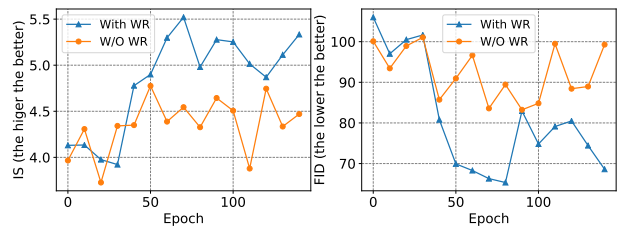


Figure 7: The curves of IS and FID during search with and without the weight-resetting (WR) strategy. (Best viewed in color)

ure, one can observe that searching with the proposed WR strategy can obtain better IS and FID scores, which demonstrates that WR strategy can effectively enhance the stability of GAN training.

5 Conclusion & Future Work

In this paper, we propose an efficient two-stage evolutionary algorithm-based NAS framework to search GANs, namely EAGAN. We demonstrate that decoupling the search of generator and discriminator can greatly improve the stability of searching GANs. The proposed weight-resetting strategy can effectively alleviate the negative impact of some generators with mode collapse when searching discriminators, and enable a fair and unbiased evaluation for different discriminators. EAGAN is very efficient and takes only 1.2 GPU days to finish the search on CIFAR-10. Our searched GANs have advanced transferability and achieve remarkable performance (IS and FID) on STL-10 datasets. In the future, we will make further improvements in the following aspects: incorporating category information into the search space, exploring high-resolution generative tasks, and finding better and cheaper metrics.

References

- Arjovsky, M.; Chintala, S.; and Bottou, L. 2017. Wasserstein GAN. *arXiv:1701.07875*.
- Bissoto, A.; Valle, E.; and Avila, S. 2019. The six fronts of the generative adversarial networks. *arXiv preprint arXiv:1910.13076*.
- Bojanowski, P.; Joulin, A.; Lopez-Pas, D.; and Szlam, A. 2018. Optimizing the Latent Space of Generative Networks. In *Proceedings of the ICML*.
- Borji, A. 2019. Pros and cons of gan evaluation measures. *Computer Vision and Image Understanding*, 179.
- Brock, A.; Donahue, J.; and Simonyan, K. 2019. Large Scale GAN Training for High Fidelity Natural Image Synthesis. In *International Conference on Learning Representations*.
- Chrabaszcz, P.; Loshchilov, I.; and Hutter, F. 2017. A down-sampled variant of imagenet as an alternative to the cifar datasets. *arXiv preprint arXiv:1707.08819*.
- Coates, A.; Ng, A.; and Lee, H. 2011. An analysis of single-layer networks in unsupervised feature learning. In *Proceedings of the fourteenth international conference on artificial intelligence and statistics*.
- Costa, V.; Lourenço, N.; and Machado, P. 2019. Coevolution of generative adversarial networks. In *International Conference on the Applications of Evolutionary Computation (Part of EvoStar)*, 473–487. Springer.
- Deb, K.; Agrawal, S.; Pratap, A.; and Meyarivan, T. 2000. A fast elitist non-dominated sorting genetic algorithm for multi-objective optimization: NSGA-II. In *International conference on parallel problem solving from nature*, 849–858. Springer.
- Doveh, S.; and Giryas, R. 2019. DEGAS: Differentiable Efficient Generator Search. *arXiv preprint arXiv:1912.00606*.
- Elsken, T.; Metzen, J. H.; and Hutter, F. 2018. Neural architecture search: A survey. *arXiv preprint arXiv:1808.05377*.
- Gao, C.; Chen, Y.; Liu, S.; Tan, Z.; and Yan, S. 2020. Adversarialnas: Adversarial neural architecture search for gans. In *Proceedings of the CVPR*.
- Gong, X.; Chang, S.; Jiang, Y.; and Wang, Z. 2019. AutoGAN: Neural Architecture Search for Generative Adversarial Networks. In *Proceedings of the ICCV*.
- Goodfellow, I.; Pouget-Abadie, J.; Mirza, M.; Xu, B.; Warde-Farley, D.; Ozair, S.; Courville, A.; and Bengio, Y. 2014. Generative adversarial nets. *Advances in neural information processing systems*, 27.
- Grnarova, P.; Levy, K. Y.; Lucchi, A.; Perraudin, N.; Goodfellow, I.; Hofmann, T.; and Krause, A. 2019. A domain agnostic measure for monitoring and evaluating gans. *Advances in Neural Information Processing Systems*, 32: 12092–12102.
- Gulrajani, I.; Ahmed, F.; Arjovsky, M.; Dumoulin, V.; and Courville, A. 2017. Improved Training of Wasserstein GANs. *arXiv:1704.00028*.
- He, H.; Wang, H.; Lee, G.-H.; and Tian, Y. 2018. Probgan: Towards probabilistic gan with theoretical guarantees. In *International Conference on Learning Representations*.
- He, X.; Zhao, K.; and Chu, X. 2021. AutoML: A survey of the state-of-the-art. *Knowledge-Based Systems*, 212.
- Heitzinger, C. 2002. *Simulation and inverse modeling of semiconductor manufacturing processes*. na.
- Heusel, M.; Ramsauer, H.; Unterthiner, T.; Nessler, B.; and Hochreiter, S. 2017. GANs Trained by a Two Time-Scale Update Rule Converge to a Local Nash Equilibrium. In *Proceedings of the NeurIPS*.
- Hjelm, R. D.; Jacob, A. P.; Che, T.; Trischler, A.; Cho, K.; and Bengio, Y. 2017. Boundary-seeking generative adversarial networks. *arXiv preprint arXiv:1702.08431*.
- Karras, T.; Aila, T.; Laine, S.; and Lehtinen, J. 2018. Progressive Growing of GANs for Improved Quality, Stability, and Variation. *arXiv:1710.10196*.
- Karras, T.; Laine, S.; and Aila, T. 2019. A style-based generator architecture for generative adversarial networks. In *Proceedings of the IEEE/CVF Conference on Computer Vision and Pattern Recognition*, 4401–4410.
- Kingma, D. P.; and Ba, J. 2014. Adam: A method for stochastic optimization. *arXiv preprint arXiv:1412.6980*.
- Krizhevsky, A.; Hinton, G.; et al. 2009. Learning multiple layers of features from tiny images. Technical report.
- LeCun, Y.; Bottou, L.; Bengio, Y.; and Haffner, P. 1998. Gradient-based learning applied to document recognition. *Proceedings of the IEEE*, 86(11): 2278–2324.
- Liu, C.; Zoph, B.; Neumann, M.; Shlens, J.; Hua, W.; Li, L.-J.; Fei-Fei, L.; Yuille, A.; Huang, J.; and Murphy, K. 2018. Progressive neural architecture search. In *Proceedings of the European conference on computer vision (ECCV)*, 19–34.
- Liu, H.; Simonyan, K.; Vinyals, O.; Fernando, C.; and Kavukcuoglu, K. 2017. Hierarchical representations for efficient architecture search. *arXiv preprint arXiv:1711.00436*.
- Liu, H.; Simonyan, K.; and Yang, Y. 2019. DARTS: Differentiable Architecture Search. In *Proceedings of the ICLR*.
- Liu, L.; Zhang, Y.; Deng, J.; and Soatto, S. 2021. Dynamically Grown Generative Adversarial Networks. *Proceedings of the AAAI Conference on Artificial Intelligence*, 35(10): 8680–8687.
- Mao, X.; Li, Q.; Xie, H.; Lau, R. Y.; Wang, Z.; and Paul Smolley, S. 2017. Least squares generative adversarial networks. In *Proceedings of the IEEE international conference on computer vision*, 2794–2802.
- Miyato, T.; Kataoka, T.; Koyama, M.; and Yoshida, Y. 2018a. Spectral Normalization for Generative Adversarial Networks. *arXiv:1802.05957*.
- Miyato, T.; Kataoka, T.; Koyama, M.; and Yoshida, Y. 2018b. Spectral normalization for generative adversarial networks. *arXiv preprint arXiv:1802.05957*.
- Odena, A.; Olah, C.; and Shlens, J. 2017. Conditional image synthesis with auxiliary classifier gans. In *International conference on machine learning*, 2642–2651. PMLR.
- Paszke, A.; Gross, S.; Massa, F.; Lerer, A.; Bradbury, J.; Chanan, G.; Killeen, T.; Lin, Z.; Gimelshein, N.; Antiga, L.; et al. 2019. Pytorch: An imperative style, high-performance deep learning library. *Advances in neural information processing systems*, 32: 8026–8037.

- Pham, H.; Guan, M. Y.; Zoph, B.; Le, Q. V.; and Dean, J. 2018. Efficient neural architecture search via parameter sharing. *arXiv preprint arXiv:1802.03268*.
- Radford, A.; Metz, L.; and Chintala, S. 2016. Unsupervised Representation Learning with Deep Convolutional Generative Adversarial Networks. arXiv:1511.06434.
- Real, E.; Aggarwal, A.; Huang, Y.; and Le, Q. V. 2019. Regularized evolution for image classifier architecture search. In *Proceedings of the AAAI*, volume 33.
- Real, E.; Moore, S.; Selle, A.; Saxena, S.; Suematsu, Y. L.; Tan, J.; Le, Q. V.; and Kurakin, A. 2017. Large-Scale Evolution of Image Classifiers. In *Proceedings of the ICML*. JMLR.org.
- Salimans, T.; Goodfellow, I.; Zaremba, W.; Cheung, V.; Radford, A.; and Chen, X. 2016. Improved Techniques for Training GANs. In *Proceedings of the NeurIPS*.
- Tian, Y.; Shen, L.; Su, G.; Li, Z.; and Liu, W. 2020a. AlphaGAN: Fully Differentiable Architecture Search for Generative Adversarial Networks. *arXiv preprint arXiv:2006.09134*.
- Tian, Y.; Wang, Q.; Huang, Z.; Li, W.; Dai, D.; Yang, M.; Wang, J.; and Fink, O. 2020b. Off-Policy Reinforcement Learning for Efficient and Effective GAN Architecture Search. In *Proceedings of the ECCV*.
- Wang, C.; Xu, C.; Yao, X.; and Tao, D. 2019. Evolutionary generative adversarial networks. *IEEE Transactions on Evolutionary Computation*, 23(6): 921–934.
- Wang, H.; and Huan, J. 2019. Agan: Towards automated design of generative adversarial networks. *arXiv preprint arXiv:1906.11080*.
- Wang, W.; Sun, Y.; and Halgamuge, S. 2019. Improving MMD-GAN Training with Repulsive Loss Function. In *International Conference on Learning Representations*.
- Wu, B.; Dai, X.; Zhang, P.; Wang, Y.; Sun, F.; Wu, Y.; Tian, Y.; Vajda, P.; Jia, Y.; and Keutzer, K. 2019. Fbnet: Hardware-aware efficient convnet design via differentiable neural architecture search. In *Proceedings of the IEEE/CVF Conference on Computer Vision and Pattern Recognition*, 10734–10742.
- Xu, Y.; Xie, L.; Zhang, X.; Chen, X.; Qi, G.-J.; Tian, Q.; and Xiong, H. 2020. PC-DARTS: Partial Channel Connections for Memory-Efficient Architecture Search. In *International Conference on Learning Representations*.
- Yang, Z.; Wang, Y.; Chen, X.; Shi, B.; Xu, C.; Xu, C.; Tian, Q.; and Xu, C. 2020. CARS: Continuous Evolution for Efficient Neural Architecture Search. In *Proceedings of the CVPR*.
- Zhang, H.; Goodfellow, I.; Metaxas, D.; and Odena, A. 2019. Self-attention generative adversarial networks. In *International conference on machine learning*, 7354–7363. PMLR.
- Zoph, B.; and Le, Q. V. 2016. Neural architecture search with reinforcement learning. *arXiv preprint arXiv:1611.01578*.
- Zoph, B.; Vasudevan, V.; Shlens, J.; and Le, Q. V. 2018. Learning transferable architectures for scalable image recognition. In *Proceedings of the IEEE conference on computer vision and pattern recognition*.